

# Gene expression analysis of dendritic cells that prevent diabetes in NOD mice: analysis of chemokines and costimulatory molecules

Penelope A. Morel,<sup>\*,†,1</sup> Mangala Srinivas,<sup>‡,2</sup> Michael S. Turner,<sup>\*</sup> Patrizia Fuschiotti,<sup>\*</sup> Rajan Munshi,<sup>§</sup> Ivet Bahar,<sup>§</sup> Maryam Feili-Hariri,<sup>\*,11,3</sup> and Eric T. Ahrens<sup>‡</sup>

Departments of <sup>\*</sup>Immunology, <sup>†</sup>Medicine, <sup>§</sup>Computational and Systems Biology, and <sup>11</sup>Surgery, University of Pittsburgh, Pittsburgh, Pennsylvania, USA; and <sup>‡</sup>Department of Biological Sciences, Carnegie Mellon University, Pittsburgh, Pennsylvania, USA

RECEIVED MARCH 8, 2011; REVISED APRIL 20, 2011; ACCEPTED MAY 5, 2011. DOI: 10.1189/jlb.0311126

## ABSTRACT

We have demonstrated previously that BM-derived DCs can prevent diabetes development and halt progression of insulinitis in NOD mice, the mouse model of type 1 diabetes. The DC population that was most effective in this therapy had a mature phenotype, expressed high levels of costimulatory molecules, and secreted low levels of IL-12p70. The protective DC therapy induced Treg and Th2 cells *in vitro* and *in vivo*. Microarray analysis of therapeutic and nontherapeutic DC populations revealed differences in the expression of OX40L, CD200, Ym-1, CCL2, and CCL5, which could play important roles in the observed DC-mediated therapy. The unique pattern of costimulatory molecules and chemokines expressed by the therapeutic DCs was confirmed by flow cytometry and ELISA. Using a novel cell-labeling and <sup>19</sup>F NMR, we observed that the chemokines secreted by the therapeutic DCs altered the migration of diabetogenic Th1 cells *in vivo* and attracted Th2 cells. These results suggest that the therapeutic function of DCs is mediated by a combination of costimulatory and chemokine properties that results in the attraction of diabetogenic Th1 and the induction of Th2 and/or Treg differentiation. *J. Leukoc. Biol.* 90: 539–550; 2011.

## Introduction

DCs play an important role in the activation and differentiation of naive T cells [1]. In particular, it has been shown that DCs can influence the differentiation of CD4<sup>+</sup> T cells into Th subsets, including Th1, Th2, Th17, and Tregs [1–4], depending on a series of factors. These factors include the dose of

antigen [5, 6], the cytokines produced by activated DCs [7–9], and the expression of specific costimulatory molecules [2, 10–12]. In general, the ability of DCs to stimulate Th1 differentiation has been correlated with the ability of DCs to produce IL-12p70, an important cytokine that drives Th1 development [9]. It has been shown that certain pathogens, such as *Schistosoma*, fail to induce IL-12p70 production and induce an alternatively matured DC capable of driving Th2 differentiation [13–15]. Certain pathogens elicit the production of IL-23 from DCs, which is important for the differentiation and maintenance of Th17 cells [2, 16]. DCs may also influence T cell responses by secreting chemokines that attract specific Th subsets.

Over the last several years, we have been studying the role of DC subsets in the pathogenesis and therapy of diabetes in NOD mice [17–19]. The NOD mouse is a murine model of autoimmune type 1 diabetes and is characterized by a period of insulinitis, followed by destruction of islets by CD4<sup>+</sup> and CD8<sup>+</sup> T cells, leading to overt diabetes. The immune system in NOD mice is skewed toward the development of Th1 responses [20], and effector Th1 cells and CTLs are responsible for the autoimmunity in NOD mice [21]. We have shown previously that a single injection of BM-derived DCs can protect young, prediabetic NOD mice from the development of diabetes [17, 18]. The therapy can be given as late as 8 weeks of age when insulinitis is already established [22] and can be effective later if the DCs are transduced to express IL-4 [22]. The therapeutic DC populations expressed high levels of costimulatory molecules (CD80, CD86, and CD40) and produced low levels of IL-12p70 following CD40 ligation [19]. Therapy with this semimature DC population altered the Th1/Th2 balance and induced a population of Th2 cells, which may be responsible for the observed protection [18]. On the other hand, an im-

Abbreviations: <sup>19</sup>F=fluorine-19, BM=bone marrow, F<sub>c</sub>=fluorine content/cell, Foxp3=forkhead box p3, GM=mouse rGM-CSF without murine rIL-4, GM4=mouse rGM-CSF with murine rIL-4, m=mouse, MBEI=model-based expression index, OX40L=OX40 ligand, PFPE=perfluoropolyether, SOM=self-organizing maps, t=time, Treg=regulatory T cell

The online version of this paper, found at [www.jleukbio.org](http://www.jleukbio.org), includes supplemental information.

1. Correspondence: Department of Immunology, University of Pittsburgh, 200 Lothrop St., BST E1048, Pittsburgh, PA 15261, USA. E-mail: [morel@pitt.edu](mailto:morel@pitt.edu)
2. Current address: Department of Tumor Immunology, Radboud University Nijmegen Medical Centre, Nijmegen, the Netherlands.
3. Current address: National Institutes of Health, National Institute of Allergy and Infectious Diseases, Bethesda, MD, USA.

mature, BM-derived DC population, which expressed low levels of costimulatory molecules and produced high levels of IL-12p70 following activation, was unable to induce protection against diabetes [18]. More recently we have observed that the therapeutic DC population can induce expansion of Tregs in the presence of low-dose antigen [6].

To identify additional molecules that would distinguish the therapeutic from the nontherapeutic DC population, we have performed microarray analysis using RNA isolated from freshly prepared DCs as well as from DCs activated by LPS + IFN- $\gamma$ . The analysis revealed many differences between the two DC populations, including the expression of specific cell-surface markers, secreted proteins, and chemokines, confirmed using flow cytometry, Luminex, and Western blot analyses. Importantly, using a novel, cell-labeling technology and quantitative  $^{19}\text{F}$  NMR analysis [23, 24], we showed that therapeutic DCs induced migration of Th1 cells toward the LN, draining the site of DC injection, and away from the pancreas. These results suggest that in addition to inducing Th2 differentiation, the therapeutic DCs in NOD mice function by altering the migration pattern of diabetogenic Th1 cells.

## MATERIALS AND METHODS

### Mice

Female NOD/Lt and NOD-SCID mice were purchased from The Jackson Laboratory (Bar Harbor, ME, USA), and NOD OX40L $^{-/-}$  and BDC2.5 TCR transgenic mice were obtained from Christophe Benoist (Harvard University, Cambridge, MA, USA). All mice were maintained in the pathogen-free animal facility of the University of Pittsburgh (Pittsburgh, PA, USA) under Institutional Animal Care and Use Committee guidelines and approved protocols.

### DC generation and flow cytometry

Myeloid progenitor cells from NOD or OX40L $^{-/-}$  BM cells were prepared as described previously by depleting MHCII $^{+}$  cells, T cells, and B cells using mAb and complement treatment [17]. The progenitor cells were cultured in the presence of rmGM-CSF (1 ng/ml; R&D Systems, Minneapolis, MN, USA) with (GM4) or without (GM) rmIL-4 (1 ng/ml; PeproTech, Rocky Hill, NJ, USA) in RPMI 1640 (Gibco, Grand Island, NY, USA) containing supplements. Cells were fed on Day 2, and DCs were purified on Day 4 using metrizamide gradients as described previously [17].

Purified Day 4 DCs were stained with FITC- or PE-conjugated mAb specific for CD80, CD86, OX40L, CD200, MHCII, and the DC marker CD11c. The DC purity was determined by the expression of DC markers and lack of staining with mAb against CD3, B220, Gr.1, and F4/80 molecules [17].

### In vitro DC:T cell cocultures

Purified, splenic CD4 $^{+}$  T cells ( $2 \times 10^5$ /ml) from NOD were cocultured with NOD DC ( $2 \times 10^5$ /ml) populations in 12-well plates for 3–4 days. Freshly isolated CD4 $^{+}$  T cells and purified T cells from primary DC:T cell cocultures were stimulated ( $0.5 \times 10^5$ /well) in a total volume of 1 ml in 24-well plates, precoated with 10  $\mu\text{g}/\text{ml}$  anti-TCR $\alpha\beta$  mAb [18]. Plates were incubated at 37°C for 2 days, and the culture supernatants were collected and kept frozen ( $-20^{\circ}\text{C}$ ). Type 1 (IFN- $\gamma$ ) and type 2 (IL-4, IL-5, IL-10) cytokines were quantified in supernatants from primary and secondary cultures by ELISA. GM4 DC from NOD or OX40L $^{-/-}$  mice and purified CD4 $^{+}$  T cells from BDC2.5 TCR transgenic mice were co-cultured in 96-well U-bottom plates. DC were seeded at  $2 \times 10^4$  cells/well and increasing doses of AV10 peptide (AVRPLWVRME) were added at least two hours

prior to the addition of CFSE-labeled CD4 $^{+}$  T cells ( $1 \times 10^5$ /well). Cells were harvested after 5 days for flow cytometric and cytokine analysis.

### Cytokine production by DC subsets

DC ( $10^6$ /ml) populations were cultured in the presence or absence of LPS (10  $\mu\text{g}/\text{ml}$ ; Sigma-Aldrich, St. Louis, MO, USA) and IFN- $\gamma$  (50 ng/ml; BD Pharmingen, San Diego, CA, USA), and supernatants were collected at various times following stimulation and kept frozen. Culture supernatants were tested for production of IL-12p70, IL-12p40, and IL-10 cytokines by ELISA, as described previously [19]. The presence of CCL5 in the supernatant was detected using a 17-plex Beadlyte kit/Luminex (Upstate, Lake Placid, NY, USA) and Luminex analysis.

### DC activation, RNA isolation, and microarray analysis

GM and GM4 DC ( $10^6$ /ml) were cultured in the presence of LPS (10  $\mu\text{g}/\text{ml}$ ; Sigma-Aldrich) and IFN- $\gamma$  (50 ng/ml; BD Pharmingen). Cells were harvested at 0, 6, and 20 h after activation, and total RNA was isolated according to the Qiagen protocol (Qiagen, Valencia, CA, USA). Each time-point was replicated two to three times; thus, a total of 15 microarrays was used for the current analysis.

The RNA labeling and microarray analysis was performed by the PittArray facility. Fragmented RNA (15  $\mu\text{g}$ ) was added to a final volume of 300  $\mu\text{l}$  hybridization cocktail (Affymetrix, Santa Clara, CA, USA). An appropriate volume of this sample was applied to the Affymetrix MG U74Av2 gene chip, and the chip was incubated overnight at 45°C with rotation. Following hybridization, the sample was removed, and the GeneChip cassette was filled with nonstringent wash buffer. The chips were loaded onto an Affymetrix Fluidics Station for wash and stain, following which, they were scanned using the GeneArray scanner.

### Data analysis

The expression level for each gene was obtained by the DNA chip analysis software, dChip v1.3 ([biosun1.harvard.edu/complab/dchip](http://biosun1.harvard.edu/complab/dchip)) [25]. The output files from the Affymetrix reader (i.e., CEL) were analyzed using dChip, and the arrays were normalized to the default baseline array (GM4 0-h sample) using the invariant set normalization algorithm implemented in dChip. The MBEI for each gene was calculated with the perfect match-only model using outlier detection and treating image spikes as single outliers. Replicate samples were pooled so that expression values for the same gene in replicate arrays were determined by considering measurement error [25]. The arrays can be found at the Gene Expression Omnibus-National Center for Biotechnology Information database (Accession Numbers GSM384656-GSM384669).

Following this low-level analysis, two different high-level analyses were performed to identify differentially expressed genes: SOM and identification of genes that are most different between the two DC subsets.

**SOM.** Genecluster2 ([www-genome.wi.mit.edu/MPR](http://www-genome.wi.mit.edu/MPR)) was used to construct SOM. The SOM method first clusters the original data in a high-dimensional space and then projects them into a lower-dimensional display space. For the present data, the original dataset of 12,488 genes was filtered to exclude transcripts with invariant expression levels across all six samples. In this manner, 1045 genes ( $\sim 8\%$ ) were obtained and organized in a  $4 \times 3$  SOM.

**Identification of genes.** The data were organized in a matrix  $A$ . Each row of  $A$  refers to one of the  $m = 12,469$  probe sets (henceforth, called genes) probed in microarrays (outlier genes excluded, as determined by dChip). The expression level for each gene  $i$  in  $A$  is represented by the MBEI obtained by dChip. The columns represent the  $n = 6$  samples, i.e., two DC populations  $\times$  three samples/population. The  $i$ th element  $a_{ik}$  of the matrix  $A$  gives the expression level of the  $i$ th gene in the  $k$ th sample, where  $1 \leq i \leq m$ , and  $1 \leq k \leq n$ . To identify genes that were differentially expressed between GM and GM4 DCs, genes, whose expression values between time-points were invariant and also, those genes with low (background-level) expression values, were eliminated.

The average expression of each gene across all 6 samples is represented by:

$$\langle \alpha_i \rangle = \frac{1}{n} \sum_{k=1}^n \alpha_{ik}$$

Additionally, genes were scored by the equation:

$$S(i) = \sum_{x=1}^3 (u_i)^2,$$

where  $S(i)$  is a measure of the change in gene expression of a gene  $i$  across all time-points,

$$u = \begin{cases} \frac{r}{r+3} & \text{if } r \geq r+3 \\ \frac{r+3}{r} & \text{if } r < r+3 \end{cases}$$

and  $r$  and  $r+3$  represent the cognate time points for each DC subset population ( $1 < r < 3$ ).

A two-step filtering strategy was used for this analysis. First, genes with  $\langle \alpha_i \rangle < 100$  units were eliminated; subsequently, genes with  $S < 8$  were excluded from further analysis. In this manner, 663 genes were obtained for additional differential expression analysis.

## Western blot analysis

DCs were prepared as described from BM cultures with GM alone or GM4. The cells ( $10^6/\text{ml}$ ) were then incubated with medium, LPS ( $10 \mu\text{g}/\text{ml}$ ), IFN- $\gamma$  ( $50 \text{ ng}/\text{ml}$ ), or LPS + IFN- $\gamma$  for 24 h. The supernatants were collected and analyzed by Western blot for the presence of Ym-1-secreted protein [26]. The supernatants were run on a SDS-PAGE gel, and Western blot was performed using a rabbit polyclonal anti-Ym-1 antibody (a kind gift of Dr. Dianne Webb, Australian National University, Canberra, Australia).

## In vitro chemotaxis assays

Supernatants from GM and GM4 DCs cultured for 24 h in medium were collected as described above. Th1 and Th2 cells were generated from purified NOD CD4 $^+$  T cells as described previously [27]. The supernatants from GM and GM4 DCs were placed in the lower wells of transwell plates, and Th1 or Th2 ( $5 \times 10^5$ ) cells were placed in the upper wells. The negative control consisted of medium, and CCL19 or CXCL12 was used as a positive control. The cells were allowed to migrate for 2 h, and the cells in the lower chamber were quantified using a Coulter counter. Each condition was run in triplicate. The migration index was calculated by dividing the number of cells that migrated in response to DC supernatant or chemokine by the number that migrated to medium alone.

## In vivo migration studies

T cells from BDC2.5 TCR transgenic mice were purified from single-cell suspensions of splenocytes using a MACS pan T cell isolation kit (Miltenyi Biotec, Auburn, CA, USA). Cells were activated in vitro by a 3-day incubation on plates coated with anti-TCR antibody in the presence of  $10 \mu\text{g}/\text{ml}$  anti-CD28 and  $10 \text{ U}/\text{ml}$  IL-2 and type 1 (anti-IL-4 mAb+IFN- $\gamma$ ) or type 2 (IL-4+anti-IFN- $\gamma$ ) cytokines, as described previously [27]. Cells were then labeled using a novel PFPE nanoemulsion reagent [28] by simple coincubation at  $37^\circ\text{C}$  for 3 h, as described elsewhere [28]. Cells were washed in PBS twice and resuspended in  $300 \mu\text{l}$  HBSS prior to transfer. In addition, some cells were pelleted and used for NMR analysis (below) to measure PFPE uptake.

Mice were injected with DCs and T cells and imaged as described previously [24]. Briefly,  $0.5 \times 10^6$ -purified NOD DCs of the appropriate subset were injected s.c. near an inguinal node into 8- to 10-week-old female NOD SCID-recipient mice. Sterile PBS was injected s.c. in the contralateral side as a control. The mice also received an i.p. injection of  $200 \text{ mg}/\text{kg}$  cyclo-

phosphamide (Sigma-Aldrich). Twenty-four hours later,  $4 \times 10^6$   $^{19}\text{F}$ -labeled NOD BDC2.5 T cells (see above) were injected i.p. Mice were killed 48 h after T cell transfer, and the pancreas, both inguinal nodes, spleen, and liver were removed and fixed in 4% paraformaldehyde in PBS prior to NMR analysis.

## $^{19}\text{F}$ NMR

One-dimensional  $^{19}\text{F}$  NMR on whole-fixed organ samples and pelleted cells was carried out using a Bruker Avance 500 MHz NMR spectrometer (Bruker BioSpin, Billerica, MA, USA). An aliquot of calibrated TFA  $^{19}\text{F}$  reference solution was added to the NMR tube with the samples [24]. First, we calibrated the amount of PFPE (i.e.,  $^{19}\text{F}$ ) taken up by the T cells after the above ex vivo-labeling procedure. Using labeled cell pellets, the average  $F_c$  was calculated by acquiring NMR spectra of a known number of PFPE-labeled cells ( $\sim 10^6$ ), spiked with a known concentration of TFA. The  $F_c$  parameter was calculated from the ratio-integrated areas of the PFPE and TFA  $^{19}\text{F}$  spectra [24]. Quantification of apparent T cell numbers in the organ and tissue samples was carried out using the measured ratio of the  $^{19}\text{F}$  spectral areas of the sample and TFA and the measured  $F_c$  parameter, as described previously [24]. All  $^{19}\text{F}$  spectra were acquired using a recycle delay of 8 s, a  $12\text{-}\mu\text{s}$  pulse width, a spectral width of 20 kHz, 256 averages, 2048 acquisition points, and a  $90^\circ$  flip angle.

## RESULTS

### NOD DC populations have distinct phenotype and function

We have shown previously that NOD DCs generated from BM cultures in GM alone or GM4 have distinct phenotypic and functional characteristics [17, 19]. Injection of young, prediabetic mice with GM4 DCs prevented the onset of diabetes, and this was characterized by an increased production of type 2 cytokines in spleen and pancreas [18, 22]. GM DCs were unable to protect NOD mice, differed from GM4 DCs, in that they expressed low levels of costimulatory molecules (ref. [19]; Fig. 1A), and produced high levels of IL-12p70 (ref. [19]; Fig. 1B). In addition, T cells cultured in the presence of GM4 DCs acquired the ability to produce type 2 cytokines, such as IL-4, IL-5, and IL-10 (Fig. 1C). In contrast, T cells cultured in the presence of GM DCs maintained the cytokine-secretion pattern of the starting population (Fig. 1C, top panel), namely, high IFN- $\gamma$ , and no type 2 cytokine production (Fig. 1C). Similar results were obtained with allogeneic T cells and with T cells from the BDC2.5 TCR transgenic NOD mouse [29] (data not shown).

### GM4 DCs have a unique pattern of gene expression

To determine whether the GM4 DC population had a gene expression pattern that might explain its ability to prevent diabetes, we performed microarray analysis and compared the GM4 DC population with nontherapeutic GM DCs. Using the SOM analysis described in Materials and Methods, 1045 genes ( $\sim 8\%$ ) were organized in a  $4 \times 3$  SOM (Fig. 2A). Each cluster comprises a subset of genes characterized by a distinctive expression profile for genes in that cluster across the six regions [30]. On inspection of the SOM, three distinct expression profiles can be distinguished: (i) clusters of genes where the expression levels in both DC populations are nearly identical (e.g., c0 and c6); (ii) clusters where expression levels between



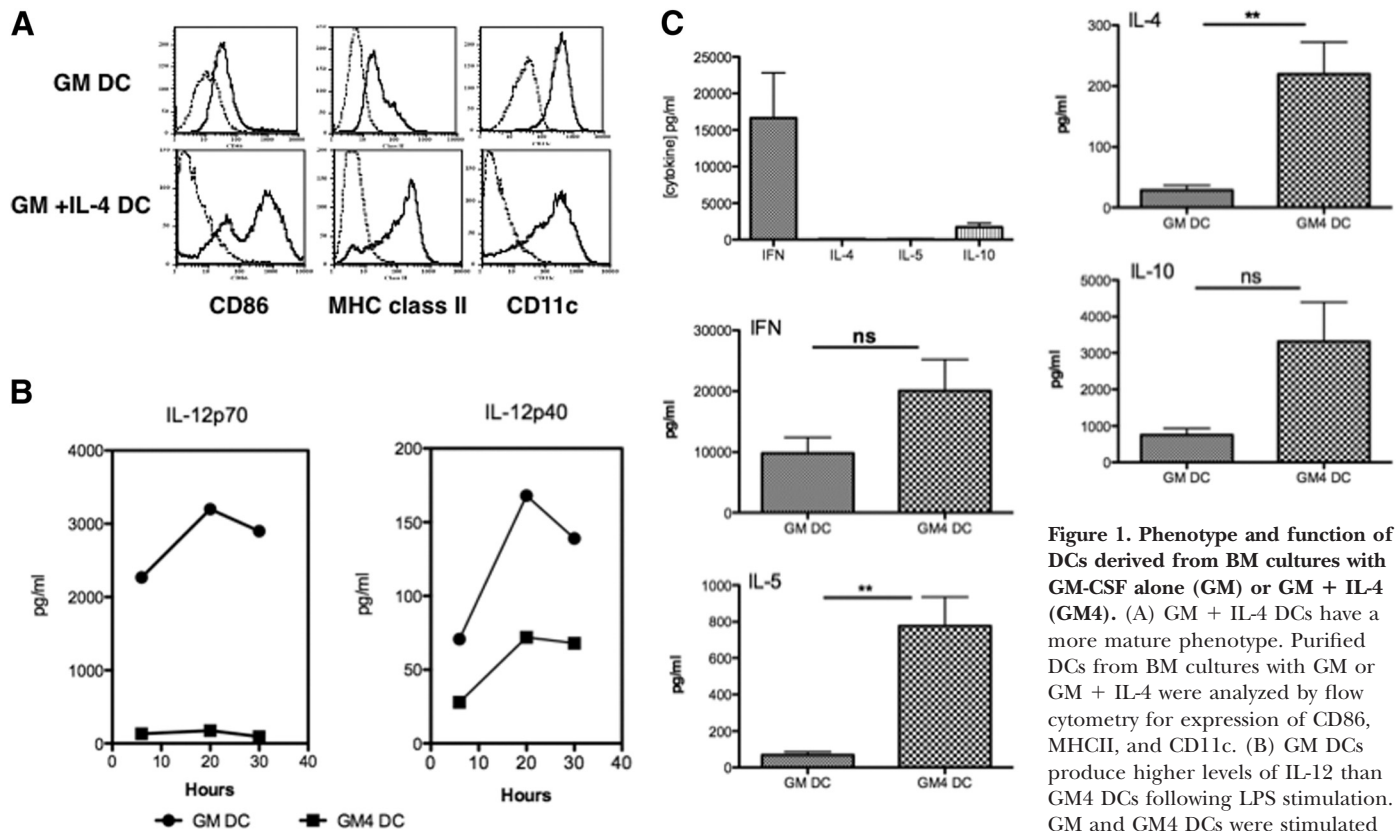


**Figure 1. Phenotype and function of DCs derived from BM cultures with GM-CSF alone (GM) or GM + IL-4 (GM4).** (A) GM + IL-4 DCs have a more mature phenotype. Purified DCs from BM cultures with GM or GM + IL-4 were analyzed by flow cytometry for expression of CD86, MHCII, and CD11c. (B) GM DCs produce higher levels of IL-12 than GM4 DCs following LPS stimulation. GM and GM4 DCs were stimulated

with LPS (10  $\mu$ g/ml) and IFN- $\gamma$  (50 ng/ml), and supernatants were collected at the indicated times. The levels of IL-12p70 (left panel) and IL-12p40 (right panel) were determined by ELISA. The results shown are representative of three independent experiments. (C) GM4 DCs induce the production of type 2 cytokines by NOD T cells. CD4<sup>+</sup> T cells were purified from the spleens of NOD mice and placed in culture with GM or GM4 DC. T cells from these cultures or freshly purified T cells were stimulated in wells coated with anti-CD3 mAb. Supernatants were collected after 48 h and tested for the presence of type 1 (IFN- $\gamma$ ) and type 2 (IL-4, IL-5, IL-10) cytokines by ELISA. The results shown represent the mean  $\pm$  SEM of six to seven independent experiments. \*\**P* values < 0.01, as determined by Student *t* test.

the two DC populations show qualitatively similar profiles (i.e., increasing or decreasing with time), the difference between the two populations being the baseline expression level (e.g., c2 and c9); and (iii) clusters of genes whose expression levels differ in the two cell populations at different time-points (e.g., c4 and c5). Particularly interesting are clusters 8–11, as these represent genes that were more highly expressed in the GM4 DC population at *t* = 0 and could therefore represent genes that played a role in the therapeutic effect of GM4 DC.

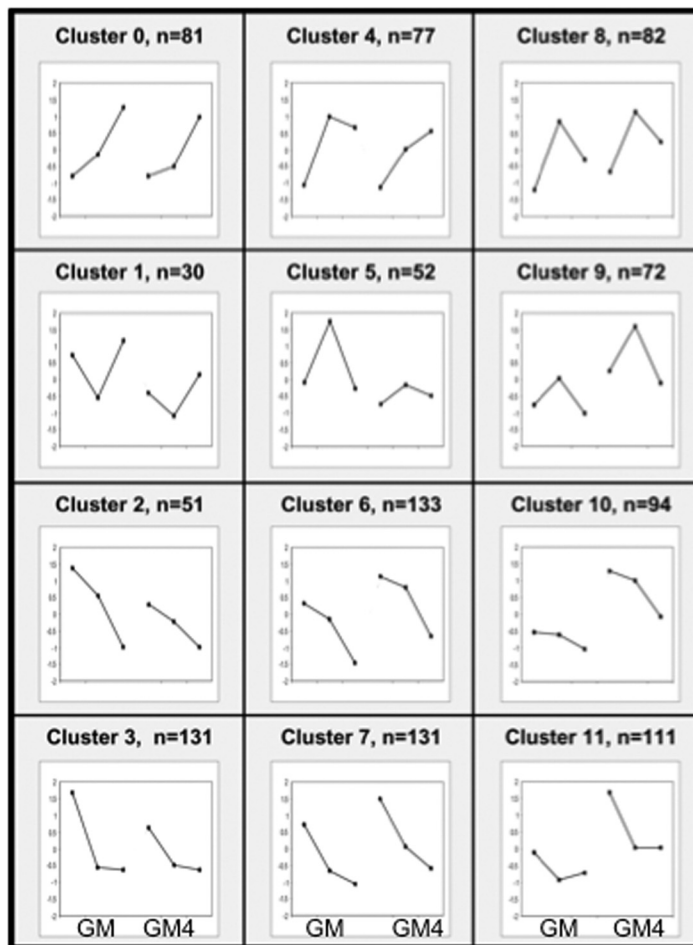
Identification of differentially expressed genes using the algorithm described in Materials and Methods revealed 663 genes that fulfilled the criteria outlined. Differences that occur at the *t* = 0 are potentially most relevant to the therapeutic effect of the DCs, as these represent DCs that were injected into NOD mice. A total of 302 of the 663 genes identified above showed changes greater than twofold between the DC subsets at *t* = 0 (Fig. 2B), and most of these changes reflect increased expression in the GM4 DC subset. Of the 302 genes, 272 genes were found in the SOM, with 156 of 272 genes in clusters 8–11 (Fig. 2B). Most of the highly expressed genes were found in clusters 10 (63/156) and 11 (49/156). A selection of these genes is shown in **Table 1**. A smaller number of genes were found to be up-regulated in GM DC at *t* = 0

(**Table 2**), and these included genes associated with the macrophage lineage, such as lysozymes, fMLPR, CD14, and the C-type lectin McI. The transcription factor Notch was more highly expressed as well as the inhibitory receptor, DC immunoreceptor. Further studies are required to determine the significance of these changes.

#### Activation of GM and GM4 DCs with LPS + IFN- $\gamma$ induces a similar pattern of gene expression

Analysis of the genes induced 6 h following activation with LPS + IFN- $\gamma$  revealed a similar pattern between DC subsets (see Supplemental file with all data). The genes that were most highly induced were chemokines, cytokines, and co-stimulatory molecules, such as CD40. Activation of both DC subsets in the presence of LPS + IFN- $\gamma$  led to the up-regulation of IL-1 $\alpha$ , IL-1 $\beta$ , IL-12p40, TNF- $\alpha$ , and the chemokines CXCL9 (monokine induced by IFN- $\gamma$ ), CXCL10 (IFN-inducible protein-10), and CXCL2 (MIP-2). In contrast, only the GM DC demonstrated an increase in IL-12p35 expression following activation, consistent with the ELISA data shown in Fig. 1. Although there were differences in the degree of up-regulation of individual genes between the DC subsets, no major differences in activation profile were observed at

A



B

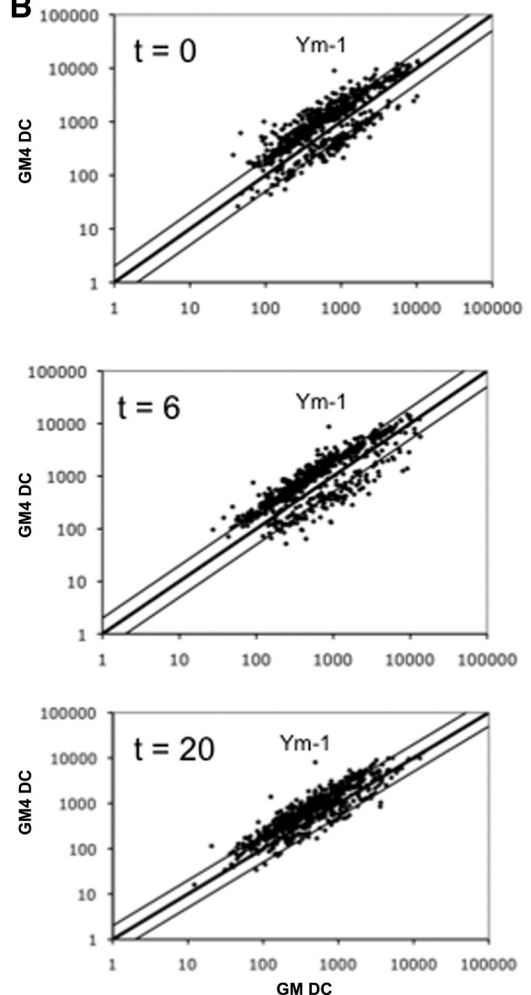


**Figure 2. Microarray analysis of GM4 DCs and GM DCs reveals differential gene expression at  $t = 0$ .** The microarrays and data analysis were performed as described in Materials and Methods, and a total of 15 microarrays is included in these results. (A) SOM of the most relevant genes was constructed using Genecluster2. The original dataset of 12,488 genes was filtered to exclude transcripts with invariant expression levels across all six samples. In this manner, 1045 genes ( $\sim 8\%$ ) were obtained, which were organized in a  $4 \times 3$  SOM. The 12 clusters are represented graphically with the number of genes in each cluster indicated at the top of each panel. In each panel, the first and second lines represent the expression pattern for GM and GM4 DCs, respectively, at 0, 6, and 20 h following LPS stimulation. The y-axis represents the normalized expression levels. (B) Six hundred sixty-three genes were identified as most differentially expressed between GM and GM4 DCs according to the algorithm defined in Materials and Methods. Plots of the expression of these genes by GM DC (x-axis) and GM4 DC (y-axis) at  $t = 0$ ,  $t = 6$ , and  $t = 20$  are shown in the indicated panels.

the 6-h time-point. We then focused our analysis on the differences observed between the DC populations at  $t = 0$ .

### Costimulatory molecules are highly expressed by GM4 DC

Several members of the costimulatory molecule family were highly expressed in GM4 DCs, including CD86, CD40, OX40L, 4-1BB, and CD200 (OX-2; Table 1). Our previous data showed that CD40 and CD86 were more highly expressed in GM4 DCs (Fig. 1) [17, 19], but the expression levels of OX40L and CD200 had not been examined previously. To confirm the microarray results for the latter, we performed flow cytometric analysis of GM and GM4 DCs (Fig. 3). OX40L and CD200 were expressed by GM4 DCs but were absent or weakly expressed on GM DCs.

The OX40/OX40L interaction has been shown to enhance Th2 development in vivo [31, 32] and in vitro [33, 34] but also to inhibit Treg differentiation [35]. Thus, we examined the role of OX40L expression on the ability of GM4 DCs to induce Treg and Th2 expansion from BDC2.5 T cells. GM4 DCs from OX40L<sup>-/-</sup> or WT NOD mice expressed similar levels of CD80, CD86, and MHCII (data not shown). We have shown recently that GM4 DCs presenting low-dose antigen lead to expansion of Tregs [6]; however, no difference in the ability of GM4 DCs from OX40L<sup>-/-</sup> or NOD mice to induce Treg expansion from BDC2.5 T cells exposed to low-dose antigen was observed (Fig. 3C). There was also no significant difference in the ability of GM4 DCs from OX40L<sup>-/-</sup> or NOD mice to induce IL-4 production in BDC2.5 T cells (Fig. 3D).

TABLE 1. List of Genes More Highly Expressed in GM4 DCs at  $t = 0$ 

Probe set	GM4	GM	FC <sup>a</sup>	SOM <sup>b</sup>	Accession number GenBank description
Costimulation/maturation markers					
103509_at	868.3	131.6	6.6	11	AA798611 4-1BB
102830_at	874.4	182.3	4.8	10	L25606 CD86
101164_at	1409.3	387.5	3.6	9	U12763 OX40L
99434_at	1439.0	419.7	3.4	10	AF001036 CD83
101851_at	1555.3	485.1	3.2	8	AF029215 CD200
97173_f_at	2244.8	751.5	3.0	10	M27134 MHC class I H2-K
101653_f_at	1115.9	397.2	2.8	10	X52914 MHC class I H2-D
99933_at	765.2	308.5	2.5	9	D26107 CD112 (nectin-2)
102655_at	236.5	95.8	2.5	9	X53176 Integrin $\alpha$ 4 (CD49d)
92962_at	462.3	192.7	2.4	8	M83312 CD40
Chemokines/chemokine receptors					
104443_at	5666.5	1322.9	4.3	9	L31580 CCR7
98406_at	9475.9	2904.4	3.3	4	AF065947 CCL5 (RANTES)
98008_at	1653.1	514.1	3.2	11	U92565 CX3CL1 (Fractalkine)
94761_at	687.7	235.7	2.9	9	X70058 CCL7 (MCP-3)
97783_at	11931.7	5513.6	2.2	6	AJ242587 CCL17 (TARC)
102736_at	1618.2	748.4	2.2	8	M19681 CCL2 (MCP-1)
102794_at	963.9	456.3	2.1	11	Z80112 CXCR4
102310_at	11406.4	6529.7	1.7	9	AF052505 CCL22 (MDC)
Secreted proteins and cytokines					
92694_at	8997.9	812.4	11.1	10	M94584 Secretory protein (YM-1)
94738_s_at	239.7	37.4	6.4	10	M33227 Defensin-related cryptdin
102218_at	589.7	136.2	4.3	8	X54542 IL-6
101551_s_at	2209.1	541.1	4.1	10	X78989 Testin
98391_at	1212.3	307.4	3.9	11	X13215 MGK-11 kallikrein
95775_f_at	1674.7	483.1	3.5	11	V00829 Kallikrein
95546_g_at	879.8	326.8	2.7	11	X04480 IGF-1
Transcription factors/signaling					
102994_at	1524.0	314.2	4.8	10	U06923 Stat4
100133_at	885.1	212.6	4.2	10	M27266 Fyn
102955_at	1703.1	409.4	4.2	11	U83148 NF-IL-3
103091_at	1683.4	543.9	3.1	10	M83380 v-rel
96651_at	496.3	163.4	3.0	10	AF035263 BAF57
92737_at	3122.8	1132.7	2.8	9	U20949 IRF-4
101465_at	461.9	168.2	2.7	8	U06924 Stat1
92832_at	1058.4	391.5	2.7	4	U88325 SOCS-1
94186_at	1902.1	742.5	2.6	8	L35302 TRAF-1
100771_at	1860.5	714.3	2.6	9	AF068182 BLNK
99475_at	3561.7	1415.0	2.5	10	U88327 SOCS-2
96260_at	1657.0	657.8	2.5	10	AB021491 P100 coactivator
100022_at	2362.1	968.9	2.4	11	D89613 CIS
98427_s_at	3918.0	1626.0	2.4	8	M57999 NF- $\kappa$ B p50
99982_at	1291.3	550.9	2.3	8	U19799 I $\kappa$ B- $\beta$
93324_at	3915.3	2123.2	1.8	10	M58566 TIS-11
Cytoskeletal proteins					
94079_at	503.6	99.4	5.1	11	X61452 Septin 4
103715_at	713.9	164.5	4.3	11	U04354 Adseverin
103462_at	469.9	157.1	3.0	11	AW122239 Dock2
94223_at	2279.0	831.7	2.7	9	AJ010045 Rho GEF
95516_at	1346.6	664.3	2.0	10	AB027290 RAB9
Other receptors and enzymes					
96918_at	1005.2	95.4	10.5	10	AI790931 Fructose bisphosphate 1
102906_at	524.6	88.2	5.9	4	L38444 TGT
99964_at	1338.5	277.0	4.8	11	AW061016 Vitamin D receptor
103554_at	1689.3	358.6	4.7	10	AA726223 Meltrin $\beta$
96515_at	3319.5	856.4	3.9	10	U70430 Fig-1
103258_at	1469.6	412.5	3.6	9	U19271 CD205 (DEC-205)
98405_at	5040.7	1682.0	3.0	9	U96700 Serpin 6

TABLE 1.(continued)

Probe set	GM4	GM	FC <sup>a</sup>	SOM <sup>b</sup>	Accession number GenBank description
99323_at	173.1	59.2	2.9	9	U64199 IL-12R $\beta$ 2
98018_at	692.2	244.8	2.8	4	L39017 Protein C receptor
92310_at	2720.1	965.4	3.8	10	M96163 Serum-inducible kinase
92401_at	1808.2	655.9	2.8	11	U27195 Leukotriene C4 synthase
103362_at	1704.0	629.1	2.7	9	D13458 Prostaglandin E receptor
96506_at	1266.1	472.1	2.6	10	D83002 Anaplastic lymphoma kinase (CD246)
93411_at	2458.4	1010.2	2.4	9	AI152789 Semaphorin 7A

<sup>a</sup>FC, Fold change. <sup>b</sup>SOM, Cluster in SOM shown in Fig. 2. Expression levels for GM4 and GM DCs. MDC, Macrophage-derived chemokine; IRF-4, IFN regulatory factor 4; SOCS-1/2, suppressor of cytokine signaling 1/2; BLNK, B cell linker protein; GEF, guanine nucleotide exchange factor; TGTP, T cell-specific GTPase.

### Expression of Ym-1 by GM4 DC

The microarray results revealed that the most differentially expressed gene by GM4 DC was Ym-1 (Fig. 2B and Table 1), and its level of expression was 11-fold higher than that seen for GM DCs. We confirmed this by performing Western blots using a polyclonal anti-Ym-1 mAb (Fig. 4). GM4 DCs produced high levels of Ym-1 in the supernatant, and this did not vary after activation, whereas GM DCs did not produce any Ym-1 before or after activation. Ym-1 has been described as a

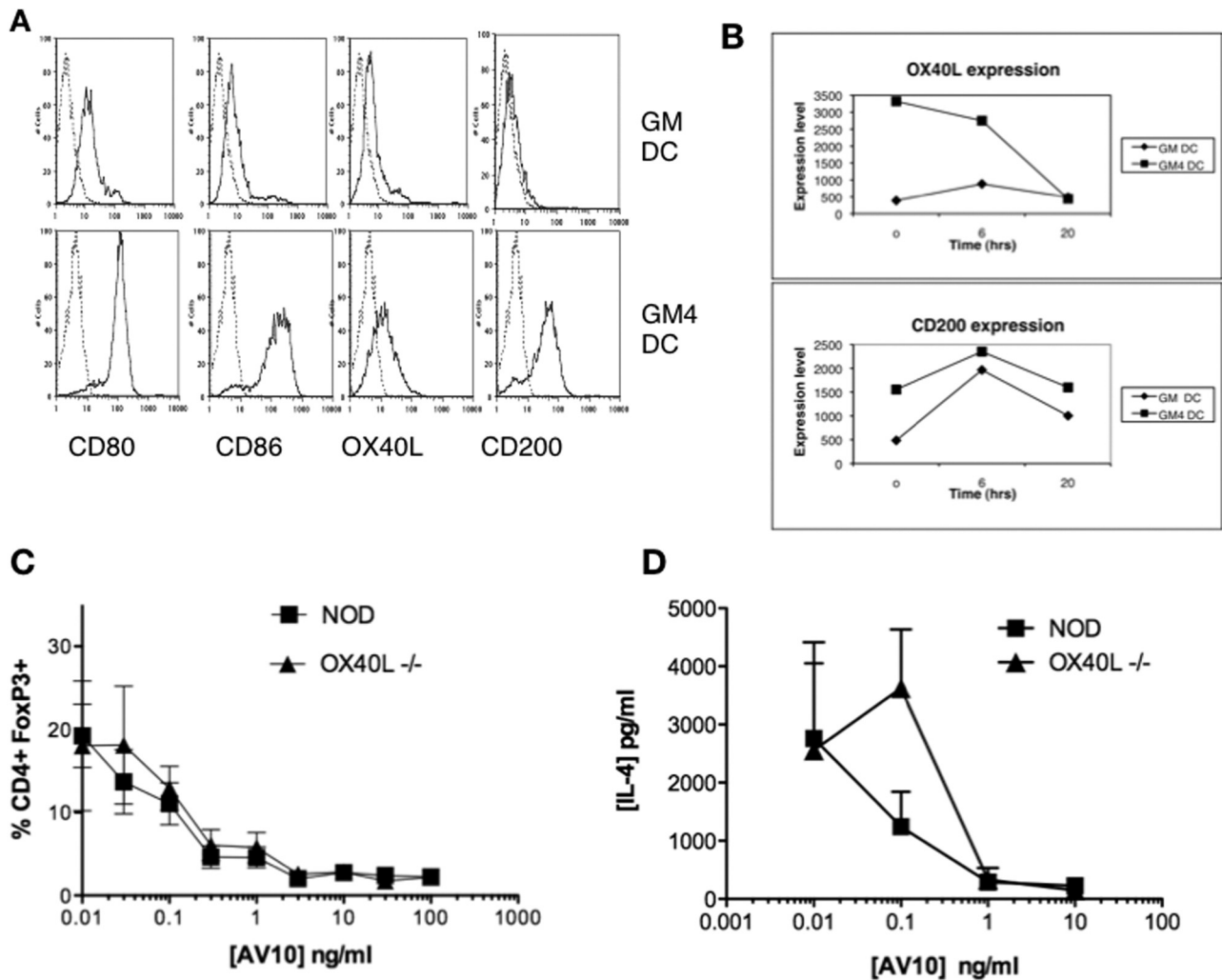
marker of alternative macrophage activation and is highly expressed in allergic lesions [26, 36], and its expression requires the presence of IL-4 and Stat6. Recent studies have suggested that Ym-1 plays a role in Th2 differentiation [37]. We have obtained several polyclonal antibodies to Ym-1, including the one used by Arora et al. [37], but we were unable to reproduce these results in our NOD system. The results obtained were contradictory, with some antibodies inhibiting IL-4 production and others enhancing IL-4 production.

Table 2. List of Genes More Highly Expressed in GM DCs at  $t = 0$ 

Probe set	GM4	GM	FC	SOM	GenBank description
95951_at	211.8	1071.9	5.1	0	AF061272 C-type lectin (McI)
160469_at	514.7	2383.4	4.6	5	M62470 Thrombospondin 1
100611_at	2443.4	9170.1	3.8	2	M211050 Lysozyme M
101800_at	183.6	632.7	3.4	4	AF072280 fMLP receptor
97497_at	355.8	1212.2	3.4	2	Z11886 Notch 1
101753_s_at	2989.4	10098.1	3.4	2	X51547 Lysozyme P
103759_at	54.8	181.2	3.3	0	D31788 CD157 (BP-3)
98088_at	1778.0	5622.5	3.2	4	X13333 CD14
92877_at	899.1	2702.8	3.0	1	L19932 TGF- $\beta$ -induced gene
97844_at	313.0	939.5	3.0	3	U67187 G-protein signaling reg RGS2
99071_at	1947.9	5734.6	2.9	5	L20315 MPS1
92762_at	518.4	1511.3	2.9	3	AJ33533 DCIR
92852_at	1171.5	3381.7	2.9	2	M18194 Fibronectin
101560_at	362.4	1031.4	2.8	5	AW061330 Embigin
96886_at	221.2	580.3	2.6	1	AW060556 Stabilin 1
100499_at	330.1	834.0	2.5	-	D29797 Syntaxin 3A
103421_at	373.7	927.1	2.5	3	D50464 SDR2
102424_at	319.3	788.5	2.5	8	J04491 CCL3
102663_at	613.0	1508.7	2.5	3	X62700 PAR-1
94792_at	755.8	1857.5	2.5	5	AI447305 Macrophage scavenger R-1
99952_at	272.9	666.2	2.4	5	X93035 Brp39
104354_at	1366.1	3291.9	2.4	1	X06368 CSF-1R
104467_at	487.9	1167.9	2.4	5	AA763004 Carboxypeptidase D
99991_at	236.5	560.7	2.4	-	U31993 IL-17R
92849_at	223.0	518.8	2.3	2	M58004 CCL6
99510_at	737.5	1707.3	2.3	3	X59274 protein kinase C $\beta$
104407_at	97.8	222.4	2.3	8	L25274 activated leukocyte CAM
94425_at	1094.1	2450.7	2.2	2	AB007599 MD-1
93871_at	1367.6	2980.7	2.2	4	L32838 IL-1ra

Expression levels for GM4 and GM DCs. BP-3, Binding protein 3; RGS2, regulator of G-protein signaling 2; MPS1, Mucopolysaccharides 1; DCIR, DC immunoreceptor; SDR2, stromal cell-derived factor receptor 2; PAR-1, protease-activated receptor-1; CAM, cellular adhesion molecule; MD-1, myeloid differentiation protein 1; IL-1ra, IL-1R antagonist.





**Figure 3. GM4 DCs express higher levels of OX40L and CD200.** (A) Flow cytometric analysis of purified GM (upper panels) and GM4 DCs (lower panels). The thin lines represent the isotype control and the thick lines, staining with the indicated antibody. The experiment shown is representative of three independent experiments. (B) Microarray results for OX40L and CD200. (C) OX40L<sup>-/-</sup> and WT DCs induce similar expansion of Tregs at low-dose antigen. BDC2.5 CD4<sup>+</sup> T cells were stimulated with NOD (■) or OX40L<sup>-/-</sup> (▲) DCs in the presence of the indicated peptide doses. After 5 days, the cells were stained for the expression of CD3, CD4, and Foxp3, and the percentage of Foxp3<sup>+</sup> cells on gated CD3<sup>+</sup> CD4<sup>+</sup> T cells is shown. Results represent mean  $\pm$  SEM of six to 10 independent experiments. (D) OX40L<sup>-/-</sup> and WT DCs induce similar levels of Th2 differentiation. BDC2.5 CD4<sup>+</sup> T cells were stimulated with NOD (■) or OX40L<sup>-/-</sup> (▲) DCs in the presence of the indicated peptide doses. After 5 days, equal numbers of cells were restimulated on anti-CD3-coated plates. Twenty-four hours later, supernatants were collected and assayed for IL-4 levels by Luminex. Results represent mean  $\pm$  SEM of two to three independent experiments. AV10, .

### The pattern of chemokine and cytokine expression differs between DC subsets

Chemokines play an important role in directing the migration of immune cells, and specific chemokines are known to attract Th2 (CCL22, CCL17), Th1 (CCL5, CCL4), Th17 (CCL22, CCL20), and Tregs (CCL22) [38]. CCL2 and CCL3 have also been shown to influence Th2 [39, 40] and Th1 [40] differentiation, respectively. The Th2-attracting chemokines CCL22, CCL2, CCL7, and CCL17 were more highly expressed by GM4 DCs than by GM DCs (Table 1). CCL5 (RANTES) and CX3CL1 (fractalkine) were also highly expressed by GM4 DCs, and these chemokines could be responsible for the recruitment of unpolarized and committed Th1 cells [41–43]. The expression

pattern for CCL5 was confirmed using Luminex analysis. We observed that GM4 DCs spontaneously produce higher levels of CCL5 (Fig. 5A), and these levels increase in both DCs following LPS stimulation (not shown). Low levels of CCL2 were detected by Luminex, and these levels rose following LPS stimulation (not shown). The complex pattern of chemokine expression with Th1 (CX3CL1, CCL5)- and Th2 (CCL2, CCL22, CCL17, CCL7)-attracting chemokines produced by GM4 DCs could be responsible for the fact that Th1 and Th2 cytokines are produced following T cell activation with GM4 DCs.

To determine whether this pattern of expression had functional consequences, we performed chemotaxis assays. In these experiments, we generated Th1 and Th2 cells from NOD



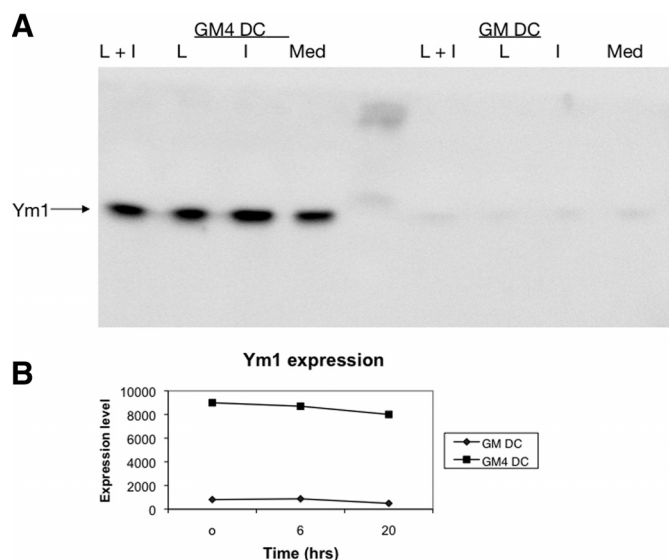


**Figure 4. GM4 DCs spontaneously secrete Ym-1.** (A) Western blot analysis of supernatants collected from GM4 and GM DCs, 24 h after stimulation with medium (Med), LPS (L), LPS + IFN- $\gamma$  (L+I), or IFN- $\gamma$  (I). The blots were probed with a polyclonal rabbit anti-Ym-1 antibody as described in Materials and Methods. The experiment shown is representative of three independent experiments. (B) Expression of Ym-1 mRNA, as detected by microarray, showing the same pattern as seen with the protein production.

CD4<sup>+</sup> T cells and placed them in the upper well of a transwell system. The lower well contained supernatants from GM or GM4 DCs. The number of T cells migrated to the lower wells after 2 h of incubation was determined by Coulter counter. Th1 and Th2 cells had significant migration in response to CCL19 but not to CXCL12 (Fig. 5B and C). Th2 cells migrated significantly toward the GM4 supernatant (Fig. 5B). There appeared to be migration of Th2 cells toward GM DCs, and Th1 cells migrated toward both DC populations, but these did not reach statistical significance (Fig. 5B and C). Similar assays were performed using sorted naïve and Tregs, but no significant migration was seen to either DC population (data not shown).

We next examined the ability of GM and GM4 DCs to influence the migration of T cells in vivo and determined whether the effects were similar to those seen in vitro. We used a novel <sup>19</sup>F NMR-based technology that we developed previously [24]. With the use of this technology, we have previously shown that activated BDC2.5 T cells can be visualized in the pancreas using MRI [24], and we examined whether GM or GM4 DCs could influence this migration pattern. We generated Th1 and Th2 cells from BDC2.5 TCR transgenic mice using a 3-day in vitro culture with skewing cytokines [27]. GM and GM4 DCs were generated from NOD BM and injected s.c. into the flank of NOD-SCID mice. One day later, the skewed BDC2.5 T cells were labeled with PFPE nanoemulsion particles, as described previously [24], and injected i.p. into the mice. After 2 days, pancreas and LNs draining the site of DC injection were removed and analyzed by <sup>19</sup>F NMR to accurately and rapidly as-

say the apparent number of T cells present in the organ. As expected, we observed the migration of Th1 and Th2 BDC2.5 T cells to the pancreas when no DCs were administered (Fig. 5D). Injection of GM or GM4 DCs did not significantly alter the pattern of T cell migration to the pancreas. No T cells were observed to accumulate in the liver or spleen (data not shown). Examination of the LNs draining the site of GM4 DC injection revealed that Th1 cells accumulated at this site, whereas Th2 cells did not (Fig. 5E). No T cells were observed in the contralateral LN (not shown) or when GM DCs were injected (not shown).

## DISCUSSION

This study demonstrates a unique pattern of gene expression by a BM-derived DC population, which prevents diabetes in NOD mice [17, 18] and induces Th2 differentiation in vivo [18] and in vitro [29]. The genes that were increased in GM4 DCs included the costimulatory molecules OX40L, CD86, CD80, CD40, and CD200, chemokines such as CCL17, CCL2, CCL5, and CCL22, and the secreted protein Ym-1. These studies also demonstrate the importance of chemokine secretion on the migration pattern of Th1 and Th2 cells in vitro and in vivo.

There has been a debate over whether the ability of DCs to induce Th1 or Th2 differentiation is determined by their lineage or by their interaction with specific pathogens and maturation factors (reviewed in refs. [1, 3, 44]). Evidence has been presented on both sides of the issue, although the consensus appears to be that the binding of pathogen-associated molecules to PRRs on the surface of DCs profoundly influences the subsequent maturation of DCs and their ability to influence Th cell differentiation [45]. In the present study, we have observed significant differences in gene expression between two DC populations that differ in their ability to protect NOD mice from the development of diabetes. Interestingly, the major differences between these DC subsets were not found following activation with the TLR4 ligand LPS but rather, were apparent prior to any maturation signal. This is important, as nonactivated GM4 DCs injected into NOD mice demonstrated a therapeutic effect [17, 18]. It is unlikely that the GM4 DCs represent a unique DC lineage, as both DC populations responded to activation with LPS + IFN- $\gamma$  in a similar manner (Fig. 2 and Supplemental data).

Costimulatory molecules have been implicated in the differentiation of Th2 cells, and it has been suggested that CD86 [12] and OX40L [46] are important for Th2 differentiation. Therapeutic GM4 DCs expressed higher levels of CD86 and OX40L, and this was seen at the gene and protein levels. A recent study by van Rijt et al. [47] demonstrated that CD80 and CD86 expression on pulmonary DCs was absolutely required for the development of Th2 responses in a model of allergic asthma. CD200 is homologous to CD80 and CD86 and has been shown to have costimulatory function [48]. In addition, blocking the interaction between CD200 and its ligand (CD200R) was recently shown to influence transplant rejection and to alter the pattern of cytokine production [49–51].

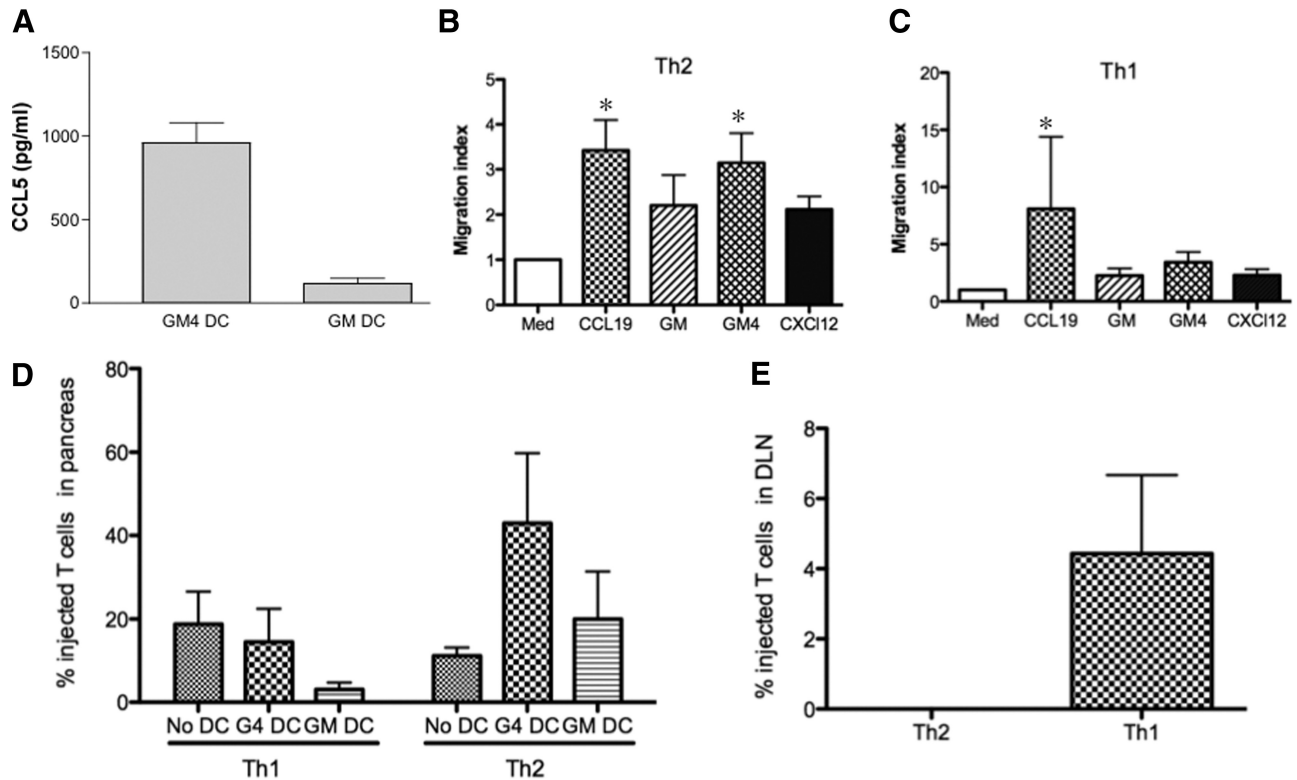


**Figure 5. GM4 DCs spontaneously produce CCL5 (RANTES) and cause in vitro migration of Th2 cells.** (A) Supernatants collected from GM4 ( $n=8$ ) and GM ( $n=5$ ) DCs after 24 h in medium were analyzed using a 17-plex Beadlyte kit/Luminex (Upstate). (B and C) Migration of Th2 (B) and Th1 (C) cells to supernatants from GM and GM4 DCs, as detected by a transwell chemotaxis assay. Th2 and Th1 cells were derived from  $CD4^+$  T cells, purified from NOD spleen, which was cultured for 3 days in type 2 or type 1 skewing conditions, respectively. Positive and negative controls were CCL19 and medium (Med), respectively. \* $P$  value  $<0.05$  as determined by ANOVA with Tukey-Kramer post test. (D) In vivo migration of Th1 cells is influenced by the presence of GM4 DCs. GM or GM4 DCs were injected ( $0.5 \times 10^6$ /mouse) into the flank of a NOD-SCID mouse. One day later, PFPE-labeled BDC2.5 Th1 and Th2 cells were injected i.p., and the pancreas and draining and nondraining LNs were analyzed by NMR. The cell quantification was based on NMR analysis of tissue samples (see Materials and Methods). NMR detection of Th1 or Th2 cell numbers in the pancreas in the absence or presence of GM4 or GM. Results represent means  $\pm$  SD of three independent experiments. (E) Detection of Th1 but not Th2 cells in the LNs draining the site of GM4 DC injection. No T cells were detected in the draining LN (DLN) adjacent to GM DC injection. Results represent means  $\pm$  SD of three independent experiments.

OX40-OX40L interactions have been shown to be important in Th2 differentiation in vivo [31, 32] and in vitro [33, 34]. The role of OX40/OX40L interactions in diabetes development has been examined recently in NOD mice [52, 53]. In these studies, OX40L $^{-/-}$  NOD mice were generated and were protected from diabetes development [52]. These mice showed more aggressive, initial activation of autoreactive T cells, but diabetes was ultimately prevented, suggesting that OX40L is required for later autoimmune islet destruction. In addition, there was no change in the cytokine balance observed in these mice. Recent studies have suggested an inhibitory role for OX40/OX40L interactions on Treg differentiation [35]. We observed no change in the ability of DCs from OX40L $^{-/-}$  mice to induce Th2 differentiation or Treg expansion. These data suggest that the therapeutic effect induced by the adoptive transfer of BM-derived DCs does not require the expression of OX40L.

The protein Ym-1 has been described recently as a product of macrophages activated by type 2 cytokines, such as IL-4 and IL-13 [54, 55]. In addition, the presence of this secreted pro-

tein has been associated with many pathological conditions associated with type 2 inflammation. Although early studies suggested that Ym-1 might function as a chemoattractant for eosinophils, this has not been confirmed in further studies. A recent study demonstrated that DCs treated with Simvastatin secreted Ym-1, which played an important role in the induction of Th2 differentiation by these DCs [37]. We were not able to reproduce these results in the NOD model, even using the same polyclonal antibody as these investigators. It is likely that the reagents available for the study of Ym-1 are not yet adequate to draw meaningful conclusions from these studies.

The pattern of chemokine production by GM and GM4 DCs, as detected by microarray, was complex, and it was not immediately clear how this would affect T cell migration. The chemokines highly expressed by GM4 DCs were of the inflammatory kind and included CCL2, CCL5, CCL17, CCL22, and CX3CL1. Analysis of protein production revealed that GM4 DCs spontaneously secreted CCL5, but only low levels of other chemokines such as CCL2 were detected by Luminex. Using an in vitro chemotaxis assay, we observed significant migration

of Th2 cells toward GM4 DCs, and although there did appear to be some migration of Th1 cells toward GM4 DCs, this was not statistically significant. In vivo migration assays using  $^{19}\text{F}$  NMR revealed that the s.c. injection of GM4 DCs attracted Th1 cells to the draining LNs, whereas GM DCs failed to do so. No Th2 cells were detected in the LNs draining the site of GM4 or GM DC injections. The apparent discrepancy between the in vitro and in vivo migration assays likely reflects differences in the time-scales involved in each technique. To detect cells by  $^{19}\text{F}$  NMR, a certain number of cells have to accumulate at a given site, and this does not capture short-term migration effects that are more readily detected with in vitro chemotactic assays.

The inability of GM DCs to attract T cells could also be related to reduced expression of CCR7, which would reduce the number of GM DCs migrating to the LN. Of note, the microarray studies revealed that GM4 DCs expressed higher levels of this receptor necessary for LN homing. Additionally, we have previously used the MRI-based technology to show that GM4 DCs migrated to the draining LN following s.c. injection [23]. In contrast, we have also shown previously that GM DCs can migrate to distant sites, such as the pancreas and spleen, following i.v. injection [17], suggesting that the lack of T cell migration to LNs draining the site of GM DC injection could be the result of a combination of factors. The constitutive expression of CCL5 by GM4 DC is likely responsible for the Th1 migration to the draining LN, as CCL5 is known to attract Th1 cells.

Chemokine secretion by DCs can also influence T cell differentiation, and it has been shown that CCL3 and CCL2 enhance IFN- $\gamma$  and IL-4, respectively [40]. The GM4 DCs in our study produce CCL2 but not CCL3, which could provide a partial explanation for their ability to induce Th2 differentiation. In addition, it has been shown that CCL2 and CCL7 but not CCL3 or RANTES inhibit IL-12p70 production from human monocytes and DCs [56]. CCL2 and CCL7 are more highly expressed by GM4 DCs compared with GM DCs, which could explain the reduced IL-12 production by GM4 DCs. Thus, the combination of chemokines that attract Th1 cells in vivo (CCL5) with chemokines that favor the production of type 2 cytokines provides some explanation for the ability of GM4 DCs to prevent diabetes in NOD mice. Preliminary experiments suggest that GM4 DCs can alter the function and phenotype of type 1-skewed T cells, suggesting that the interaction between diabetogenic Th1 cells and therapeutic GM4 DCs could reduce the diabetogenic potential of these cells.

In conclusion, GM4 DCs express several molecules that could be responsible for their ability to prevent diabetes in NOD mice and induce Th2 responses. These include specific costimulatory molecules, secreted proteins, and chemokines. Here, we have reported a pattern of chemokine expression that correlates with differential migration of disease-promoting Th1 cells and tolerogenic Th2 cells. Further studies are under way to elucidate the precise role that these pathways play in the therapeutic function of GM4 DCs.

## AUTHORSHIP

P.A.M. designed the experiments, interpreted the data, and wrote the paper. M.S., under the direction of E.T.A., performed the in vivo migration studies and NMR analysis in Fig. 5 and contributed to data interpretation and writing of the paper. M.S.T. performed the OX40L $^{-/-}$  experiments in Fig. 3, assisted M.S. in the generation of DCs and T cells for the in vivo migration studies, and contributed to data interpretation and paper editing. P.F. performed the Ym-1 studies in Fig. 4 and the in vitro migration studies in Fig. 5 and contributed to editing the paper. R.M., under the direction of I.B., performed the analysis of the microarray data described in Fig. 2. M.F.H. performed the characterization of DCs shown in Fig. 1, generated the RNA for microarray analysis, and contributed to the experimental design, data interpretation, and manuscript preparation. E.T.A. developed the  $^{19}\text{F}$  cell-labeling technology and directed the in vivo migration studies in Fig. 5.

## ACKNOWLEDGMENTS

This work was supported by NIH grant CA73743 and American Diabetes Association grant 1-06-RA-94 to P.A.M. and NIH grants EB03453 and CA134633 and the Pittsburgh NMR Center for Biomedical Research, which is supported by P41-EB001977 to E.T.A. M.S.T. was supported by NIH training grant T32CA82084. We acknowledge expert technical help from Dewayne Falkner.

## REFERENCES

1. Kapsenberg, M. L. (2003) Dendritic-cell control of pathogen-driven T-cell polarization. *Nat. Rev. Immunol.* **3**, 984–993.
2. Perona-Wright, G., Jenkins, S. J., O'Connor, R. A., Zienkiewicz, D., McSorley, H. J., Maizels, R. M., Anderton, S. M., MacDonald, A. S. (2009) A pivotal role for CD40-mediated IL-6 production by dendritic cells during IL-17 induction in vivo. *J. Immunol.* **182**, 2808–2815.
3. Pulendran, B., Smith, J. L., Caspary, G., Brasel, K., Pettit, D., Maraskovsky, E., Maliszewski, C. R. (1999) Distinct dendritic cell subsets differentially regulate the class of immune response in vivo. *Proc. Natl. Acad. Sci. USA* **96**, 1036–1041.
4. Rissoan, M. C., Soumelis, V., Kadowaki, N., Grouard, G., Briere, F., de Waal Malefyt, R., Liu, Y. J. (1999) Reciprocal control of T helper cell and dendritic cell differentiation. *Science* **283**, 1183–1186.
5. Boonstra, A., Asselin-Paturel, C., Gillet, M., Crain, C., Trinchieri, G., Liu, Y. J., O'Garra, A. (2003) Flexibility of mouse classical and plasmacytoid-derived dendritic cells in directing T helper type 1 and 2 cell development: dependency on antigen dose and differential Toll-like receptor ligation. *J. Exp. Med.* **197**, 101–109.
6. Turner, M. S., Kane, L. P., Morel, P. A. (2009) Dominant role of antigen dose in CD4 $^{+}$ Foxp3 $^{+}$  regulatory T cell induction and expansion. *J. Immunol.* **183**, 4895–4903.
7. De Smedt, T., Van Mechelen, M., De Becker, G., Urbain, J., Leo, O., Moser, M. (1997) Effect of interleukin-10 on dendritic cell maturation and function. *Eur. J. Immunol.* **27**, 1229–1235.
8. Kaliński, P., Hilkens, C. M., Wierenga, E. A., Kapsenberg, M. L. (1999) T-cell priming by type-1 and type-2 polarized dendritic cells: the concept of a third signal. *Immunol. Today* **20**, 561–567.
9. Macatonia, S. E., Hosken, N. A., Litton, M., Vieira, P., Hsieh, C. S., Culpepper, J. A., Wysocka, M., Trinchieri, G., Murphy, K. M., O'Garra, A. (1995) Dendritic cells produce IL-12 and direct the development of Th1 cells from naive CD4 $^{+}$  T cells. *J. Immunol.* **154**, 5071–5079.
10. Kim, M. Y., Bekiaris, V., McConnell, F. M., Gaspal, F. M., Raykundalia, C., Lane, P. J. (2005) OX40 signals during priming on dendritic cells inhibit CD4 T cell proliferation: IL-4 switches off OX40 signals enabling rapid proliferation of Th2 effectors. *J. Immunol.* **174**, 1433–1437.
11. MacDonald, A. S., Straw, A. D., Dalton, N. M., Pearce, E. J. (2002) Cutting edge: Th2 response induction by dendritic cells: a role for CD40. *J. Immunol.* **168**, 537–540.



12. Ranger, A. M., Prabhu Das, M., Kuchroo, V. K., Glimcher, L. H. (1996) B7-2 (CD86) is essential for the development of IL-4-producing cells. *Int. Immunol.* **8**, 1549–1560.
13. Favreuw, C., Gosset, P., Bureau, F., Angeli, V., Hirai, H., Maruyama, T., Narumiya, S., Capron, M., Trottein, F. (2003) Prostaglandin D2 inhibits the production of interleukin-12 in murine dendritic cells through multiple signaling pathways. *Eur. J. Immunol.* **33**, 889–898.
14. Jankovic, D., Kullberg, M. C., Caspar, P., Sher, A. (2004) Parasite-induced Th2 polarization is associated with down-regulated dendritic cell responsiveness to Th1 stimuli and a transient delay in T lymphocyte cycling. *J. Immunol.* **173**, 2419–2427.
15. Trottein, F., Pavelka, N., Vizzardelli, C., Angeli, V., Zouain, C. S., Pelizzola, M., Capozzoli, M., Urbano, M., Capron, M., Belardelli, F., Granucci, F., Ricciardi-Castagnoli, P. (2004) A type I IFN-dependent pathway induced by *Schistosoma mansoni* eggs in mouse myeloid dendritic cells generates an inflammatory signature. *J. Immunol.* **172**, 3011–3017.
16. Korn, T., Bettelli, E., Oukka, M., Kuchroo, V. K. (2009) IL-17 and Th17 cells. *Annu. Rev. Immunol.* **27**, 485–517.
17. Feili-Hariri, M., Dong, X., Alber, S. M., Watkins, S. C., Salter, R. D., Morel, P. A. (1999) Immunotherapy of NOD mice with bone marrow-derived dendritic cells. *Diabetes* **48**, 2300–2308.
18. Feili-Hariri, M., Falkner, D. H., Morel, P. A. (2002) Regulatory Th2 response induced following adoptive transfer of dendritic cells in prediabetic NOD mice. *Eur. J. Immunol.* **32**, 2021–2030.
19. Feili-Hariri, M., Morel, P. A. (2001) Phenotypic and functional characteristics of BM-derived DC from NOD and non diabetes-prone strains. *Clin. Immunol.* **98**, 133–142.
20. Koarada, S., Wu, Y., Ridgway, W. M. (2001) Increased entry into the IFN- $\gamma$  effector pathway by CD4<sup>+</sup> T cells selected by I-Ag7 on a nonobese diabetic versus C57BL/6 genetic background. *J. Immunol.* **167**, 1693–1702.
21. Wang, B., Gonzalez, A., Benoist, C., Mathis, D. (1996) The role of CD8<sup>+</sup> T cells in the initiation of insulin-dependent diabetes mellitus. *Eur. J. Immunol.* **26**, 1762–1769.
22. Feili-Hariri, M., Falkner, D. H., Gambotto, A., Papworth, G. D., Watkins, S. C., Robbins, P. D., Morel, P. A. (2003) Dendritic cells transduced to express IL-4 prevent diabetes in nonobese diabetic mice with established insulinitis. *Hum. Gene Ther.* **14**, 13–23.
23. Ahrens, E. T., Flores, R., Xu, H., Morel, P. A. (2005) In vivo imaging platform for tracking immunotherapeutic cells. *Nat. Biotechnol.* **23**, 983–987.
24. Srinivas, M., Morel, P. A., Ernst, L. A., Laidlaw, D. H., Ahrens, E. T. (2007) Fluorine-19 MRI for visualization and quantification of cell migration in a diabetes model. *Magn. Reson. Med.* **58**, 725–734.
25. Li, C., Wong, W. H. (2003) DNA-chip analyzer (dChip). In *The Analysis of Gene Expression Data: Methods and Software* (G. Parmigiani, E. S. Garrett, R. Irizarry, S. L. Zeger, eds.), Springer, New York, NY, USA.
26. Webb, D. C., McKenzie, A. N., Foster, P. S. (2001) Expression of the Ym2 lectin-binding protein is dependent on interleukin (IL)-4 and IL-13 signal transduction: identification of a novel allergy-associated protein. *J. Biol. Chem.* **276**, 41969–41976.
27. Chen, X. P., Falkner, D. H., Morel, P. A. (2005) Impaired IL-4 production by CD8<sup>+</sup> T cells in NOD mice is related to a defect of c-Maf binding to the IL-4 promoter. *Eur. J. Immunol.* **35**, 1408–1417.
28. Janjic, J. M., Srinivas, M., Kadayakkara, D. K., Ahrens, E. T. (2008) Self-delivering nanoemulsions for dual fluorine-19 MRI and fluorescence detection. *J. Am. Chem. Soc.* **130**, 2832–2841.
29. Feili-Hariri, M., Falkner, D. H., Morel, P. A. (2005) Polarization of naive T cells into Th1 or Th2 by distinct cytokine-driven murine dendritic cell populations: implications for immunotherapy. *J. Leukoc. Biol.* **78**, 656–664.
30. Tamayo, P., Slonim, D., Mesirov, J., Zhu, Q., Kitareewan, S., Dmitrovsky, E., Lander, E. S., Golub, T. R. (1999) Interpreting patterns of gene expression with self-organizing maps: methods and application to hematopoietic differentiation. *Proc. Natl. Acad. Sci. USA* **96**, 2907–2912.
31. Hoshino, A., Tanaka, Y., Akiba, H., Asakura, Y., Mita, Y., Sakurai, T., Takaoka, A., Nakaike, S., Ishii, N., Sugamura, K., Yagita, H., Okumura, K. (2003) Critical role for OX40 ligand in the development of pathogenic Th2 cells in a murine model of asthma. *Eur. J. Immunol.* **33**, 861–869.
32. Linton, P. J., Bautista, B., Biederman, E., Bradley, E. S., Harbertson, J., Kondrack, R. M., Padrick, R. C., Bradley, L. M. (2003) Costimulation via OX40L expressed by B cells is sufficient to determine the extent of primary CD4 cell expansion and Th2 cytokine secretion in vivo. *J. Exp. Med.* **197**, 875–883.
33. de Jong, E. C., Vieira, P. L., Kalinski, P., Schuitmaker, J. H., Tanaka, Y., Wierenga, E. A., Yazdanbakhsh, M., Kapsenberg, M. L. (2002) Microbial compounds selectively induce Th1 cell-promoting or Th2 cell-promoting dendritic cells in vitro with diverse Th cell-polarizing signals. *J. Immunol.* **168**, 1704–1709.
34. Ito, T., Wang, Y.-H., Duramad, O., Hori, T., Delespesse, G. J., Watanabe, N., Qin, F. X.-F., Yao, Z., Cao, W., Liu, Y.-J. (2005) TSLP-activated dendritic cells induce an inflammatory T helper type 2 cell response through OX40 ligand. *J. Exp. Med.* **202**, 1213–1223.
35. So, T., Croft, M. (2007) Cutting edge: OX40 inhibits TGF- $\beta$  and antigen-driven conversion of naive CD4 T cells into CD25<sup>+</sup> Foxp3<sup>+</sup> T cells. *J. Immunol.* **179**, 1427–1430.
36. Arora, S., Hernandez, Y., Erb-Downward, J. R., McDonald, R. A., Toews, G. B., Huffnagle, G. B. (2005) Role of IFN- $\gamma$  in regulating T2 immunity and the development of alternatively activated macrophages during allergic bronchopulmonary mycosis. *J. Immunol.* **174**, 6346–6356.
37. Arora, M., Chen, L., Paglia, M., Gallagher, L., Allen, J. E., Vyas, Y. M., Ray, A., Ray, P. (2006) Simvastatin promotes Th2-type responses through the induction of the chitinase family member Ym1 in dendritic cells. *Proc. Natl. Acad. Sci. USA* **103**, 7777–7782.
38. Bromley, S. K., Mempel, T. R., Luster, A. D. (2008) Orchestrating the orchestrators: chemokines in control of T cell traffic. *Nat. Immunol.* **9**, 970–980.
39. Gu, L., Tseng, S., Horner, R. M., Tam, C., Loda, M., Rollins, B. J. (2000) Control of TH2 polarization by the chemokine monocyte chemoattractant protein-1. *Nature* **404**, 407–411.
40. Karpus, W. J., Lukacs, N. W., Kennedy, K. J., Smith, W. S., Hurst, S. D., Barrett, T. A. (1997) Differential CC chemokine-induced enhancement of T helper cell cytokine production. *J. Immunol.* **158**, 4129–4136.
41. Fraticelli, P., Sironi, M., Bianchi, G., D'Ambrosio, D., Albanesi, C., Stoppacciaro, A., Chieppa, M., Allavena, P., Ruco, L., Girolomoni, G., Sinigaglia, F., Vecchi, A., Mantovani, A. (2001) Fractalkine (CX3CL1) as an amplification circuit of polarized Th1 responses. *J. Clin. Invest.* **107**, 1173–1181.
42. Luther, S. A., Cyster, J. G. (2001) Chemokines as regulators of T cell differentiation. *Nat. Immunol.* **2**, 102–107.
43. Zou, W., Borvak, J., Marches, F., Wei, S., Galanaud, P., Emilie, D., Curiel, T. J. (2000) Macrophage-derived dendritic cells have strong Th1-polarizing potential mediated by  $\beta$ -chemokines rather than IL-12. *J. Immunol.* **165**, 4388–4396.
44. Shortman, K., Liu, Y. J. (2002) Mouse and human dendritic cell subtypes. *Nat. Rev. Immunol.* **2**, 151–161.
45. Pulendran, B., Tang, H., Denning, T. L. (2008) Division of labor, plasticity, and crosstalk between dendritic cell subsets. *Curr. Opin. Immunol.* **20**, 61–67.
46. Liu, Y. J. (2007) Thymic stromal lymphopoietin and OX40 ligand pathway in the initiation of dendritic cell-mediated allergic inflammation. *J. Allergy Clin. Immunol.* **120**, 238–244, quiz 245–246.
47. van Rijt, L. S., Jung, S., Kleinjan, A., Vos, N., Willart, M., Duez, C., Hoogsteden, H. C., Lambrecht, B. N. (2005) In vivo depletion of lung CD11c<sup>+</sup> dendritic cells during allergen challenge abrogates the characteristic features of asthma. *J. Exp. Med.* **201**, 981–991.
48. Borriello, F., Lederer, J., Scott, S., Sharpe, A. H. (1997) MRC OX-2 defines a novel T cell costimulatory pathway. *J. Immunol.* **158**, 4548–4554.
49. Gorczynski, R. M. (2006) Thymocyte/splenocyte-derived CD4<sup>+</sup>CD25<sup>+</sup>Treg stimulated by anti-CD200R2 derived dendritic cells suppress mixed leukocyte cultures and skin graft rejection. *Transplantation* **81**, 1027–1034.
50. Gorczynski, R. M., Chen, Z., Yu, K., Hu, J. (2001) CD200 immunoadhesion suppresses collagen-induced arthritis in mice. *Clin. Immunol.* **101**, 328–334.
51. Minas, K., Liversidge, J. (2006) Is the CD200/CD200 receptor interaction more than just a myeloid cell inhibitory signal? *Crit. Rev. Immunol.* **26**, 213–230.
52. Martin-Orozco, N., Chen, Z., Poirot, L., Hyatt, E., Chen, A., Kanagawa, O., Sharpe, A., Mathis, D., Benoist, C. (2003) Paradoxical dampening of anti-islet self-reactivity but promotion of diabetes by OX40 ligand. *J. Immunol.* **171**, 6954–6960.
53. Pakala, S. V., Bansal-Pakala, P., Halteman, B. S., Croft, M. (2004) Prevention of diabetes in NOD mice at a late stage by targeting OX40/OX40 ligand interactions. *Eur. J. Immunol.* **34**, 3039–3046.
54. Nair, M. G., Cochrane, D. W., Allen, J. E. (2003) Macrophages in chronic type 2 inflammation have a novel phenotype characterized by the abundant expression of Ym1 and Fizz1 that can be partly replicated in vitro. *Immunol. Lett.* **85**, 173–180.
55. Welch, J. S., Escoubet-Lozach, L., Sykes, D. B., Liddiard, K., Greaves, D. R., Glass, C. K. (2002) TH2 cytokines and allergic challenge induce Ym1 expression in macrophages by a STAT6-dependent mechanism. *J. Biol. Chem.* **277**, 42821–42829.
56. Braun, M. C., Lahey, E., Kelsall, B. L. (2000) Selective suppression of IL-12 production by chemoattractants. *J. Immunol.* **164**, 3009–3017.

KEY WORDS:  
diabetes • T cells • chemotaxis • microarray analysis